Resonance Raman/Absorption Characterization of the Oxo Intermediates of Cytochrome *c* Oxidase Generated in Its Reaction with Hydrogen Peroxide: pH and H_2O_2 Concentration Dependence

Denis A. Proshlyakov,[‡] Takashi Ogura,[‡] Kyoko Shinzawa-Itoh,[§] Shinya Yoshikawa,[§] and Teizo Kitagawa*[,‡]

Graduate University for Advanced Studies and Institute for Molecular Science, Okazaki National Research Institutes, Myodaiji, Okazaki, 444 Japan, and Department of Life Science, Faculty of Science, Himeji Institute of Technology, 1479-1 Kanaji, Kamigoricho, Akogun, Hyogo 678-12, Japan

Received September 5, 1995; Revised Manuscript Received March 26, 1996[⊗]

ABSTRACT: Effects of pH and H_2O_2 concentration on the reaction of cytochrome *c* oxidase (CcO) with H_2O_2 were studied with the high-performance Raman/absorption simultaneous determination technique reported previously (Proshlyakov et al., 1996). This reaction generates two intermediates called 607- and 580-nm forms, and we found that they show the same oxygen-isotope-sensitive RR bands as those of the intermediates in O_2 reduction by CcO. In transient absorption spectra obtained under single turnover conditions, the 607-nm form appeared as the primary intermediate and subsequently the 580-nm and resting forms, suggesting that H_2O_2 serves as an oxidant for the resting enzyme but as a reductant for both the 607- and 580-nm forms in the peroxide cycle. The rise rate of absorption at 607 nm was insensitive to the H_2O/D_2O exchange, but the decay was significantly slower in D_2O than in H_2O. With the microcirculating system, each intermediate was maintained at a constant level under steady-state conditions by supplying H_2O_2 continuously. In the pH range between 7.4 and 10.0, the population of the 607-nm form decreased at higher pH and at higher concentrations of H_2O_2. The Fe═O stretching ($\nu_{Fe=O}$) frequencies of the oxo heme of the 607-nm form, observed at 804/769 cm^{-1} for their $H_2{}^{16}O_2/H_2{}^{18}O_2$ derivatives, were unaltered in this pH range and exhibited a D_2O/H_2O shift even at pH 10.0. This indicates that the iron-bound oxygen is hydrogen-bonded to a distal residue in this pH range. When the 580-nm form is dominant under the nonsaturating level of H_2O_2, two other oxygen-isotope-sensitive Raman bands have been observed at 785/750 cm^{-1} and 355/340 cm^{-1} at neutral pH, but the former disappeared above pH 8.5 and the latter above pH 9.0 without significant changes of absorption spectra, suggesting the presence of two separate species in the name of the 580-nm form. However, under the saturating concentration of H_2O_2, these Raman bands were unaltered between pH 7.4 and 10.0. In contrast, in the absence of excess peroxide, no oxygen-isotope-sensitive RR bands were observed despite dominance of the 580-nm form. The disappearance of these Raman bands demonstrates the occurrence of oxygen exchange between the oxo heme and bulk water, whose rate surpasses the formation rate of the 580-nm form at alkaline pH and/or at low H_2O_2 concentration. Such an oxygen exchange did not take place in the 607-nm form. Under the identical experimental conditions for generating a particular steady state, the exchange of H_2O with D_2O caused significant depopulation of the 580-nm form and concomitant increase of the 607-nm form. This was satisfactorily interpreted in terms of the difference in the decay rate of the 607-nm form between H_2O and D_2O. Thus, the reduction of the 607-nm form to the 580-nm form is likely to be a key step of the redox-linked proton pumping in the O_2 reduction.

Cytochrome *c* oxidase (CcO)[1] (EC1.9.3.1) is the terminal enzyme of the mitochondrial electron transfer chain and catalyzes reduction of molecular oxygen to water (Babcock & Wikström, 1992). The reaction takes place at the Fe_{a3}/Cu_B binuclear center and is coupled with proton translocation across the inner membrane (Wikström et al., 1981; Chan & Li, 1990; Babcock & Wikström, 1992), while this enzyme contains another two redox-active metal centers as Fe_a and Cu_A. The vectorial proton translocation may require protein conformational changes to take place (Malmström, 1985) at the expense of the energy released upon dioxygen reduction, which would in turn involve structural rearrangements at the oxygen binding site. The enzymatic reaction with O_2 proceeds via several intermediates.

On the other hand, reactions of oxidized CcO with hydrogen peroxide have been extensively studied with visible absorption spectroscopy and it is suggested that some intermediates are common to those involved in the O_2 reduction (Bickar et al., 1982; Kumar et al., 1984; Wrigglesworth, 1984; Gorren et al., 1986; Vygodina & Konstantinov, 1988). The peroxide intermediates are named in terms of the maximum absorption wavelength in the difference spectra with regard to the resting enzyme, and the presence of two intermediates, at least, has been established, that is, 607- and 580-nm forms.[2] Both forms have a similar Soret band with the maximum at 428 nm (Gorren et al., 1986; Weng & Baker, 1991; Fabian & Palmer, 1995) and the change from the resting enzyme to the 607-nm form exhibits an isosbestic

* Author to whom correspondence should be addressed.
‡ Okazaki National Research Institutes.
§ Himeji Institute of Technology.
⊗ Abstract published in *Advance ACS Abstracts,* June 1, 1996.
[1] Abbreviations: RR, resonance Raman; CcO, cytochrome *c* oxidase; HRP, horseradish peroxidase; CcP, cytochrome *c* peroxidase.

S0006-2960(95)02096-4 CCC: $12.00

point at 425 nm. Due to the similarity of the Soret band, Weng and Baker (1991) and Fabian and Palmer (1995) assumed that the 607- and 580-nm forms have an identical oxidation state, whereas Orii (1988) suggested that the 607- and 580-nm forms correspond to the peroxy and ferryl intermediates in O_2 reduction, respectively. Clarification of this controversy by other techniques is desirable.

Resonance Raman (RR) spectroscopy has been acknowledged as a powerful technique for studying the structure−function relationship of various heme proteins (Kitagawa, 1986; Spiro, 1988). Its application to the reaction of reduced CcO with O_2 allowed identification of several intermediates on the basis of the observation of oxygen-isotope-sensitive RR bands. The primary intermediate gives the Fe-O_2 stretching band ($\nu_{Fe\text{-}O2}$) at 571 cm^{-1} and the final intermediate gives the Fe-OH stretching band ($\nu_{Fe\text{-}OH}$) at 450 cm^{-1}. This is in general consensus, but three other oxygen-isotope-sensitive bands (804, 785, and 355 cm^{-1}), which are observed for middle intermediates between the primary and final intermediates (Han et al., 1990; Vartosis et al., 1993; Ogura et al., 1993), are still under debate.

Recently we have applied a high-performance Raman/absorption simultaneous determination technique to the intermediates in the reaction of oxidized CcO with H_2O_2 (Proshlyakov et al., 1996) and detected three oxygen-isotope-sensitive Raman bands identical to those of the middle intermediates of this enzyme in the O_2 reduction. In other words, H_2O_2 produces these physiological intermediates of O_2 reduction under different conditions, particularly under the extremely slow electron supply in the [H_2O_2 + oxidized CcO] reaction, compared with the physiological reaction. Thus, the [H_2O_2 + oxidized CcO] system provides a unique opportunity for investigation of the structure and function of these middle intermediates. It should be noted that the resonance Raman data are the only chemical evidence so far obtained for demonstrating importance of the [H_2O_2 + oxidized CcO] reaction in the physiological meaning. In this study, we have investigated pH and H_2O_2 concentration dependence of intermediates of the peroxide reaction by the use of the high-performance Raman/absorption simultaneous determination technique.

MATERIALS AND METHODS

Cytochrome *c* oxidase was purified from bovine heart as described previously (Yoshikawa et al., 1977), concentrated to ∼500 μM, and stored on ice or in liquid nitrogen until use. The enzyme solution was diluted with 100 mM sodium phosphate or borate buffer of a desired pH to the final concentration of 50 or 10 μM (in terms of cytochrome aa_3 units) for spectral measurements. $H_2{}^{16}O_2$ (30%, Wako Chemicals, Osaka, Japan) was used as purchased, while synthesis of $H_2{}^{18}O_2$ was described elsewhere (Hashimoto et al., 1984). The stock solutions of hydrogen peroxide were made 100 or 50 mM and were stored frozen until use.

The Raman/absorption simultaneous measurements were carried out under steady-state conditions using the microcirculating system reported previously (Proshlyakov et al., 1996). The linear flow rate of the sample in the cell was 2.8 m/s. Optimum conditions for generating a desired steady state were adjusted for each preparation of the enzyme by monitoring absorption spectrum, because the distribution of intermediates depended sensitively on the enzyme preparation.

Raman scattering was excited at 427 nm unless otherwise stated, and the laser power of excitation beam (diameter = 15−20 μm) was 2.5 or 7.5 mW for 50 and 10 μM enzyme solutions, respectively, at the sample point (quartz flow cell, cross section = 0.6 × 0.6 mm^2). Spectra of intermediates in the steady state were measured for 40 min using a fresh sample for each isotope; array records for every exposure of 0.5−1 min were stored in a two-dimensional array for each isotope and subsequently the spectra in the two-dimensional array were integrated to one-dimensional array over the desired period of time (not necessarily from the start of reaction). The data were acquired and processed on a personal computer with an original program xD Soft (by D.P.). All the Raman spectra shown in this study are normalized by the intensity of the porphyrin ν_7 band at 683 cm^{-1} assuming a linear baseline between 550 and 820 cm^{-1}.

Transient absorption spectra were measured using a Jasco UV900 spectrophotometer equipped with a photodiode array detector (Hamamatsu linear image sensor, C2327). The detector was managed by a personal computer. A 30-W xenon arc lamp (Hamamatsu Photonics) was used as a light source, the total power of which was less than 0.5 mW at the sample. The data were acquired in the 500−700-nm range (600 pixels) at the fastest rate (33 ms/spectrum) and stored in a two-dimensional matrix. The reference spectra were measured just before the reaction was started. Difference absorption spectra were subsequently calculated each time. Smoothing of spectra were carried out with the binomial smoothing algorithm (Marchand & Marmet, 1983) and practically performed by a built-in function of the Igor program (Wave Metrics Inc.). All absorption spectra observed will be given as difference spectra with regard to the resting state.

RESULTS

Figure 1 shows the simultaneously determined Raman/absorption spectra of reaction intermediates of CcO with hydrogen peroxide in the pH range between 6.0 (F and F′) and 10.0 (A and A′) obtained in the presence of H_2O_2 at a nonsaturating level (medium concentration). The RR spectra (Figure 1, left) are represented in a form of isotope-difference spectrum ($H_2{}^{16}O_2$ derivative minus $H_2{}^{18}O_2$ derivative). Since the porphyrin modes insensitive to oxygen-isotope substitution compensate each other, only the vibrations involving movements of the bound oxygen atom remain in the difference spectrum. Previous studies at neutral pH (Proshlyakov et al., 1996) have established that the 607-nm form gives rise to the oxygen-isotope-sensitive RR bands at 804/769 cm^{-1} for intermediates with $H_2{}^{16}O_2/H_2{}^{18}O_2$ and the 580-nm form gives two couples of RR bands at 785/750 and 355/340 cm^{-1}. These bands are in fact seen in trace E, but their intensities are varied with pH.

The absorption spectra (Figure 1, right) indicate that the 580-nm form is relatively more populated at higher pH but

[2] The derivative of CcO with maxima at 607 and 570 nm in the difference absorption spectrum *versus* the resting enzyme is referred as the 607-nm form in this study and is distinguished from the 580-nm form, which is characterized by the maxima at 580−585 and 530−535 nm in the difference spectrum. This terminology does not reflect the oxidation state of the enzyme. This is used instead of so-called peroxy and ferryl compounds to avoid confusion with the oxidation state.

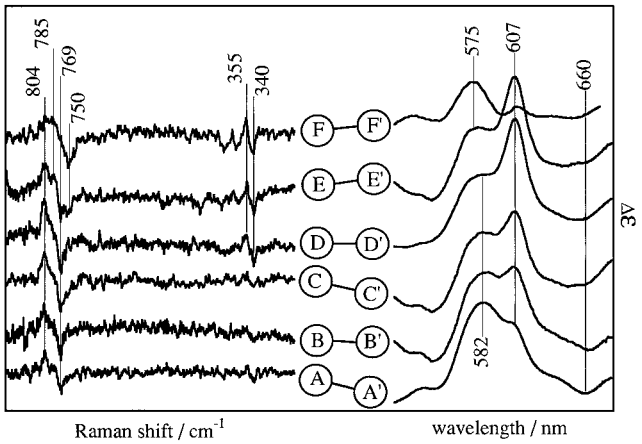

FIGURE 1: pH dependence of simultaneously determined Raman/absorption spectra of CcO reaction intermediates with hydrogen peroxide in the steady states: A/A′, pH = 10.0; B/B′, pH = 9.5; C/C′, pH = 9.0; D/D′, pH = 8.5; E/E′, pH = 7.4; and F/F′, pH = 6.0. Traces A−F denote the difference Raman spectra ([$H_2{}^{16}O_2$ derivative] − [$H_2{}^{18}O_2$ derivative]): ordinate full scale, 0.2 of the ν_7 band in the raw spectra; resolution, ∼1 cm^{-1}/channel; accumulation time, 2 × 2400 s for each isotope for traces A, B, C, and E. Traces A′−F′ denote the corresponding difference absorption spectra (intermediates − resting enzyme): integration 2400 s; path length, 0.6 mm; ordinate full scale, $\Delta\epsilon$ = 15.0 mM^{-1} cm^{-1}. All absorption spectra were measured simultaneously with corresponding Raman spectra. The CcO concentration was 50 μM. The relative rates of slow addition of H_2O_2 were (A/A′) = (B/B′) < (C/C′) = (D/D′) = (E/E′) < (F/F′).

is gradually replaced by the 607-nm form as the pH decreases until pH 7.4. Below this pH there is a large change and the 607-nm form disappears, leaving a peak at 575 nm at pH 6.0. In the RR spectra, the intensity of the 804/769 cm^{-1} bands increased in accord with the intensity increase of the 607-nm band. The 785/750-cm^{-1} bands can be seen at pH 7.4 (E) but not above pH 8.5 (A−D). The 355/340-cm^{-1} bands can be clearly seen below pH 8.5 (D−F) but do not appear above pH 9.0 (A−C). Because all the Raman/absorption spectra in Figure 1 were observed under similar rates of peroxide addition, these spectral differences are attributed solely to the pH difference. The different pH dependences of the 785/750- and 355/340-cm^{-1} bands indicate that they arise from separate molecular species. However, the absence of the 785/750- and 355/340-cm^{-1} bands at alkaline pH in spite of the high population of the 580-nm form is to be elucidated.

Figure 2 shows the results obtained under turnover conditions above pH 8.5 at the saturating concentration of H_2O_2. Contrary to the case of Figure 1, the 785/750- and 355/340-cm^{-1} bands are observed at the same frequencies and intensities in the pH range from 10.0 to 8.5. In consonance with the Raman spectra, the 580-nm band was observed with no detectable intensity near 607 nm at any pH examined, although showing some distortion in the base line.[3] These Raman and visible spectral properties resemble

[3] Partial precipitation of enzyme occurs on the wall of the cell in the laser beam at high peroxide concentration and high pH and causes irregular distortion of the baseline in the absorption measurements. Due to this reason the absorption spectrum could not be integrated over the whole period of Raman accumulation (40 min) in some cases. However, when possible, Raman and absorption spectra were measured simultaneously for 10 min or longer, and they were assumed to correspond to each other.

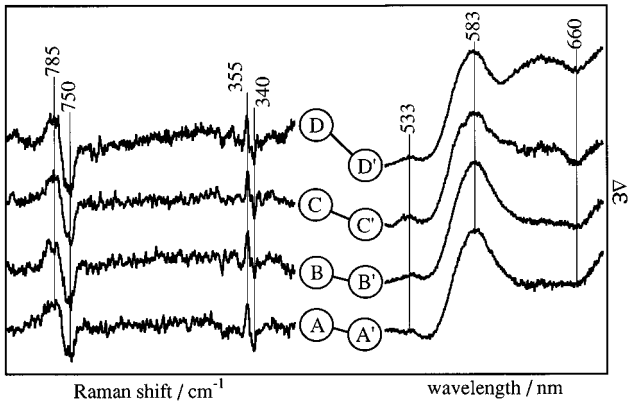

FIGURE 2: Insensitivity of the 580 nm form of CcO to pH under steady-state conditions with high concentrations of hydrogen peroxide: A/A′, pH = 10.0; B/B′, pH = 9.5; C/C′, pH = 9.0; D/D′, pH = 8.5. Traces A−D denote the difference Raman spectra: ordinate full scale, 0.3 of the ν_7 band in the raw spectra; accumulation time, 1 × 2400 s for each isotope for traces A−C. Traces A′−D′ show the corresponding difference absorption spectra: ordinate full scale, $\Delta\epsilon$ = 15.0 mM^{-1} cm^{-1}; spectra A′ and B′ were obtained by integration[3] over first 600 s and spectra C′ and D′ over all 2400 s of the corresponding Raman measurements. The CcO concentration was 10 μM. Other conditions were the same as those for Figure 1.

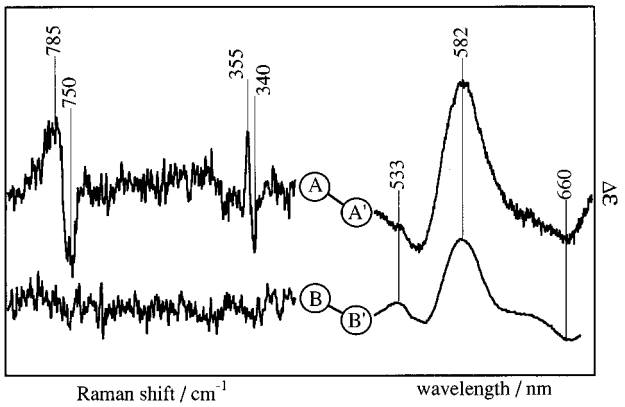

FIGURE 3: Raman/absorption spectra of the 580 nm form of CcO at pH 10.0 obtained at high concentrations (A/A′) and in the absence (B/B′) of hydrogen peroxide. Traces A and B denote Raman spectra: ordinate full scale, 0.1 of the ν_7 band in the raw spectrum; accumulation time, 2400 s (trace A) and 2 × 1800 s (trace B) for each isotope. Traces A′ and B′ denote the simultaneously observed absorption spectra: ordinate full scale, $\Delta\epsilon$ = 8.3 mM^{-1} cm^{-1}; spectrum A′ was integrated[3] over first 600 s; a linear base line was assumed between 515 and 630 nm for both spectra. Enzyme concentration was 10 and 50 μM for spectra A/A′ and B/B′, respectively. Spectra B/B′ were obtained in the presence of catalase as described in Materials and Methods. Other conditions were the same as those for Figure 1.

those at pH 6.0 in the presence of the medium concentration of H_2O_2 (Figure 1F).

The results shown in Figures 1 and 2 suggest that the appearance of the 785/750- and 355/340-cm^{-1} RR bands at alkaline pH depends on the peroxide concentration. Accordingly, we tried to remove excess H_2O_2 from the medium after the reaction. Traces B and B′ in Figure 3 show the visible absorption and Raman spectra of the 580-nm form in the absence of H_2O_2 at pH 10.0, which was prepared by adding catalase (50 units/mL) after complete development of the 580-nm form at the saturating concentration of H_2O_2. The Raman and absorption spectra in the presence of excess amounts of H_2O_2 taken from Figure 2 are also shown as

traces A and A′ for comparison. The visible absorption spectra in the two extreme cases of the H_2O_2 concentration are indistinguishable from each other. The 580-nm form in the absence of H_2O_2 thus obtained was stable under ambient temperature and slowly degraded to the fully oxidized form without yielding any new intermediates ($t_{1/2} = 40-60$ min). However, no RR band was observed in the absence of H_2O_2. This strongly suggests that the heme-bound oxygen atom of the 580-nm form is exchangeable with that of bulk water at alkaline pH and apparent Raman intensities of the 785/750- and 355/340-cm^{-1} bands are determined as a result of competition between the formation of new isotope-labeled 580-nm form with $H_2{}^{18}O_2$ and the oxygen exchange reaction with $H_2{}^{16}O$.[4] No such strong dependence on peroxide concentration was found for the intensities of the two Raman bands at pH 7.4, where the 580-nm form yielded detectable RR bands at 785/750 and 355/340 cm^{-1} irrespective of the concentrations of H_2O_2 (Proshlyakov et al., 1996). These results indicate that at lower pH, the 580-nm form is regenerated at the rate faster than the oxygen exchange reaction, as if the effective H_2O_2 concentration were increased.

When the oxidized enzyme was treated with a limited amount of H_2O_2, the 580-nm form, once formed, decayed much faster than in the absence of H_2O_2 as stated above and was replaced transiently with the 607-nm form at both neutral and alkaline pHs (results not shown). These results together with the observations shown in Figures 1 and 2, which indicate that the 607-nm form was completely replaced with the 580-nm form under saturating amounts of H_2O_2, demonstrate that H_2O_2 participates both in the decay of the 580-nm form to the oxidized form and in the formation of the 580-nm form from the 607-nm form as an electron donor.

The 804/769-cm^{-1} bands of the 607-nm form at neutral pH were previously assigned to the Fe═O stretching mode ($\nu_{Fe=O}$) of an oxo heme using $H_2{}^{16}O^{18}O$ and Raman excitation at 607 nm (Proshlyakov et al., 1994). Simulation calculations for the observed spectra revealed that the $\nu_{Fe=O}$ frequency was higher by 1.3 cm^{-1} in D_2O than in H_2O. Therefore, the iron-bound oxygen atom was deduced to be hydrogen-bonded to some nearby residue at neutral pH. The $\nu_{Fe=O}$ frequency at alkaline pH in Figure 1 is identical with that at neutral pH, suggesting that the hydrogen bond is retained at pH 10.0. To confirm this, similar measurements were carried out with D_2O solutions at pD 10.0. The intermediates were generated under the same conditions, but as shown in Figure 4, the absorption spectrum obtained with D_2O (spectrum A′) was distinctly different from that obtained with H_2O (spectrum B′). To examine possible effects of laser illumination on the sample, parallel absorption measurements without laser illumination were performed and the obtained spectra are displayed by traces C and D in Figure 4 for D_2O and H_2O, respectively. Spectra C and D for D_2O and H_2O are virtually identical with spectra A′ and B′, respectively, indicating little effect of laser illumination on the state of sample. The shoulder at 607 nm in spectrum B′ was replaced with an intense band in spectrum A′, and the small but characteristic band at 535 nm disappeared upon substitution of H_2O with D_2O.

[4] Preliminary experiments showed that the oxygen atom of the 580-nm form is in fact exchangeable with bulk water at pH 10 in the absence of excess peroxide.

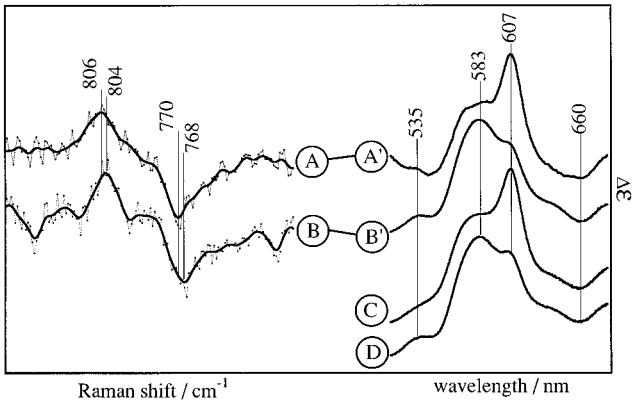

FIGURE 4: Effects of H/D isotope substitution of solvent on the steady-state Raman/absorption spectra of CcO intermediates at pH/pD 10.0. Spectra A/A′ and B/B′ were obtained with D_2O and H_2O, respectively, under otherwise the same conditions. Dots in traces A and B denote the observed points of $H_2{}^{16}O_2/H_2{}^{18}O_2$ difference Raman spectra in the 800-cm^{-1} region, and broken lines denote the connection of dots. Solid lines denote the experimental spectra smoothed using binomial algorithm (9 passes); ordinate full scale, 0.115 and 0.057 of the ν_7 band in the raw spectra for traces A and B, respectively. Accumulation time, 3 × 2400 s for $H_2{}^{16}O_2$ and 2 × 2400 s for $H_2{}^{18}O_2$ for trace A, and 4 × 2310 s for each isotope of trace B. Trace A′ was measured simultaneously with trace A, and trace B′ was obtained by averaging of 12 selected spectra along the corresponding Raman measurements. Spectra C and D were measured for the D_2O and H_2O solutions, respectively, for intermediates obtained with $H_2{}^{16}O_2$ in the absence of laser illumination; accumulation time, 2400 s each; ordinate full scale, $\Delta\epsilon$ = 13.4 mM^{-1} cm^{-1}. Other conditions were the same as those in Figure 1.

The RR spectra observed simultaneously with absorption spectra A′ and B′ are depicted by traces A and B in Figure 4, respectively, in which dots (and associated broken lines) and solid lines denote the observed points and smoothed spectra, respectively. The smoothing was carried out using binomial algorithm (9 passes). The two RR spectra are alike, but the 804/769-cm^{-1} bands in H_2O seem to be upshifted in D_2O by ca. 2 cm^{-1}. The small upshifts of these bands in D_2O were reproducibly observed in all the measurements performed. This is in agreement with the previous results obtained with red excitation (+1.3 cm^{-1}; Proshlyakov et al., 1994). The RR spectrum of the CcO intermediates in D_2O solution at pD 10.0 obtained with red excitation (not shown) was very close to that observed for the neutral solution (Proshlyakov et al., 1994). All these data indicate that the 804-cm^{-1}/607-nm form of CcO at pH 10.0 is identical with the one at neutral pH.

To get an insight into the large changes in the absorption spectrum induced by the H_2O/D_2O exchange, the [H_2O_2 + oxidized CcO] reaction was pursued by transient absorption spectra. As explained under Materials and Methods, the absorption spectra between 500 and 700 nm were observed every 32 ms. Figure 5 depicts the difference absorbance at 607 nm against time in D_2O, pD 10.0 (trace A), in H_2O, pH 10.0 (trace B), and in H_2O, pH 8.5 (trace C) under otherwise identical conditions. The experimental profiles were smoothed using binomial algorithm (3 passes). The data were analyzed with a model of sequential unimolecular irreversible reactions, that is, $X_1 \rightarrow X_2 \rightarrow X_3$, in which the initial concentrations of X_2 and X_3 were made zero as the boundary conditions. Here the peak height differences between the H_2O and D_2O solutions in Figure 5 were adjusted by the initial concentration of X_1.

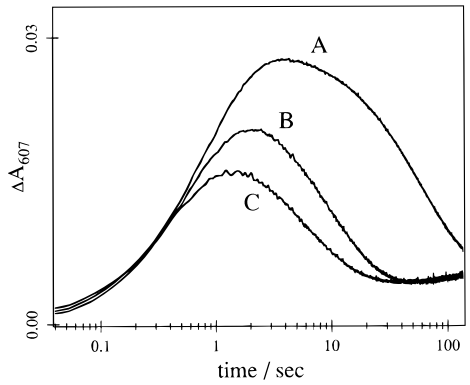

FIGURE 5: Effects of pH and H_2O/D_2O substitution of solvent on the kinetics of the peroxide reaction. Difference absorbances at 607 nm are plotted against time for the solutions of D_2O, pD 10.0 (A), H_2O, pH 10.0 (B), and H_2O, pH 8.5 (C). The sample contained 0.6 mL of 7.5 μM CcO in 100 mM sodium borate buffer. Reaction was started by rapid injection (~30 ms) of 6 μL of 0.4 M stock solution of hydrogen peroxide. Reaction was carried out aerobically at ambient temperature. Path length, 10 mm. Empirical baseline was drawn between 517 and 630 nm in the original absorbance versus wavelength spectra and was used in the estimation of absorbance at individual wavelengths. The experimental profiles were smoothed using binomial algorithm (3 passes).

The first-order rate constants for the exponential rise rates of the 607-nm form were deduced from these calculations to be 1.2, 1.5, and 2.3 s^{-1} for traces A, B, and C, respectively. No intermediate species was observed prior to the 607-nm form. The decay rate constants were 0.015, 0.10, and 0.15 s^{-1} for traces A, B, and C, respectively. The slower decay rate at pD 10.0 compared with that at pH 10.0 is highly likely to cause higher population of the 607-nm species in D_2O under steady-state conditions. The shift of steady-state distribution of intermediates upon the H_2O/D_2O exchange was apparently similar to that observed upon a pH decrease from 10.0 to 8.5 (Figure 1). However, in Figure 5 the rise and decay rates of the 607-nm forms are not significantly altered between pH 10.0 and 8.5, suggesting that other steps become faster upon lowering of pH.

DISCUSSION

Effects of pH and H_2O_2 Concentration on the Reaction of Cytochrome c Oxidase with H_2O_2. The experimental results given above concerning the effects of H_2O_2 concentration and pH on the peroxide reaction suggest the following mechanism. The oxidized CcO reacts with H_2O_2 as an oxidant to yield the 607-nm form as the first detectable intermediate. Then, H_2O_2 reduces the 607-nm form to the 580-nm form, which is further reduced by H_2O_2 to the oxidized CcO, most likely, via the Fe^{3+}-OH form. Lowering pH increases the overall reactivity of CcO with H_2O_2 so that the visible spectral changes with pH resemble those induced by changes in H_2O_2 concentrations. The 607-nm form has a Raman band at 804 cm^{-1}, and the 580-nm form contains two species, one with the Raman band at 785 cm^{-1} and the other at 355 cm^{-1}. The former two bands are due to Fe═O stretching vibrations and the latter are due to the bending mode of the His─Fe═O group. The oxo oxygens of the 785- and 355-cm^{-1} species are exchangeable with oxygen atoms of bulk water to abolish the effect of oxygen isotope substitution in H_2O_2, when the formations of these species are slower than their exchanges. The absorption and Raman spectral characteristics of the 607- and 580-nm forms and their properties are summarized in Table 1, where the oxidation level is represented with the terminology for O_2 reduction.

Nature of the Three Intermediate Species. We have shown previously that the 607-nm form has an oxo heme whose oxygen atom is hydrogen-bonded to some residue in the heme pocket at neutral pH (Proshlyakov et al., 1994). In the case of HRP compound II the removal of the hydrogen bond between distal histidine and the oxygen atom of ferryl oxo heme at alkaline pH resulted in the upshift of the $\nu_{Fe=O}$ frequency by ca. 13 cm^{-1} from 774−775 cm^{-1} (pH 7) up to 787−789 cm^{-1} (pH 11) (Hashimoto et al., 1984; Sitter et al., 1985; Terner et al., 1985; Hashimoto et al., 1986 a,b). Accordingly, an appreciable upshift of this mode of the 607-nm form would be expected if the hydrogen bond was broken at alkaline pH. The present study shows that the frequencies of the 804/769-cm^{-1} bands and their H_2O/D_2O substitution sensitivity remain unaltered at pH 10, suggesting the presence of the hydrogen bond up to pH 10. It implies that the pK_a of the hydrogen-bond donor is higher than 10.

The presence of a hydrogen bond in HRP compound II at neutral pH results in a rapid exchange of an oxygen atom between the oxo heme and bulk water. The exchange reaction ceased to take place at alkaline pH (Hashimoto et al., 1986 a,b). The rapid exchange is also evident for CcP compound ES (Hashimoto et al., 1986c; Reczek et al., 1989). The 804/769-cm^{-1} RR bands indicate no oxygen exchange with bulk water in spite of the presence of the hydrogen bonding, contrary to the peroxidases mentioned above.

So far it has been believed that the 580-nm form denotes a single ferryl oxo intermediate. In the previous report, however, we showed that two distinct oxygen-isotope-sensitive bands appearing in the RR spectrum of the 580-nm form are assignable to two separate ferryl oxo intermediates (Proshlyakov et al., 1996), namely, that the bands at 785/750 cm^{-1} were assigned to the $\nu_{Fe=O}$ mode of one form of ferryl oxo intermediate and the bands at 355/340 cm^{-1} were tentatively assigned to a His─Fe═O bending mode of another form. The effect of pH on the RR spectra at the medium concentration of H_2O_2 examined in this study (Figure 1) supports that the 785/750- and 355/340-cm^{-1} bands arise from different species which exhibit definitely different pH dependences about the exchange of bound oxygen. The broad feature of the 785/750-cm^{-1} bands might be due to the presence of the second Fe═O stretching mode arising from the 355/340-cm^{-1} species very near the 785/750-cm^{-1} band.

The 355-cm^{-1} band was apparently associated with the 804-cm^{-1} band in the O_2 reduction but with the 785-cm^{-1} band in the H_2O_2 reaction. This discrepancy is likely to be due to the difference in the efficiency of the electron supply to the Fe_{a3}─Cu_B site in the two systems. It should be noted that the investigation of the H_2O_2 reaction, which is not a physiological process, revealed the independency of the 355-cm^{-1} species.

Involvement of the Protonated Groups. The present study suggests that two types of protonated groups are involved in the reaction of oxidized CcO with hydrogen peroxide. The first type includes an amino acid residue(s) which donates a hydrogen bond to the oxo oxygen of the 804-cm^{-1} species. The pK_a of the hydrogen donor should be higher than 10, and the presence of a tyrosine residue near Fe_{a3}, revealed by mutagenesis studies (Hosler et al., 1993), suggests that

Table 1: Spectral Characteristics of Intermediates in the Reaction of Oxidized Cytochrome *c* Oxidase with Hydrogen Peroxide

			absorption spectra λ_{max} values (nm)			Raman spectra			
species	oxidation level[a]	favorable conditions	Soret[b]	α[b]	difference[c]	$^{16}O/^{18}O$[d] (cm^{-1})	assignment	observable at medium [H_2O_2]	observable at high [H_2O_2]
607 nm	$2e^-$ (peroxy)	neutral pH, low [H_2O_2]	428	601	607	804/769	$\nu_{Fe=O}$	$7 < pH \leq 10$	N[e]
580 nm	$3e^-$ (ferryl)	high pH, high [H_2O_2]	428	597	~580	355/340	$\delta_{Fe=O}$	$pH < 9$	$pH \leq 10$
						785/750	$\nu_{Fe=O}$	$pH < 8.5$	$pH \leq 10$

[a] $2e^-$ and $3e^-$ denote two- and three-electron reduced states of dioxygen and correspond to the peroxy (or P) and ferryl (or F) states, respectively. [b] Absolute spectra (Gorren et al., 1986; Weng & Baker, 1991). [c] Difference spectra *versus* resting enzyme. [d] Characteristic oxygen isotope-sensitive Raman bands for $H_2{}^{16}O_2/H_2{}^{18}O_2$. [e] Not populated under steady-state conditions.

the hydrogen-bond donor could be a tyrosine OH. The hydrogen atom involved in the H-bond could be utilized as the scalar proton. This oxo oxygen was not exchangeable with oxygen of bulk water in contrast to HRP compound II and CcP compound ES, as stated above. The oxo oxygens of the 785- and 355-cm^{-1} species, which were exchangeable with bulk water, suggest, in analogy to the above enzymes, the presence of the hydrogen bond donated by a surrounding amino acid residue similar to the 804-cm^{-1} species. The presence of the hydrogen bond may facilitate the reverse reaction from the Fe^{3+}-OH to the Fe^{4+}═O···H. This would explain the oxygen exchangeability of the oxo oxygen through Fe^{3+}-OH, which should be readily exchanged with bulk water. The lack of oxygen exchangeability of the 804-cm^{-1} band may be due to the irreversibility of the reduction of the 607-nm form to the 580-nm form. In this regard the present observations contradict the proposal that the 607- and 580-nm forms are in a chemical equilibrium in the same oxidation state (Fabian & Palmer, 1995). In addition to the irreversibility, the apparent exchangeability of the oxygen atom can also be affected by the protein structure, which controls the diffusion of bulk water coming in/going out of the proximity of the oxo heme.

$H_2{}^{16}O/H_2{}^{18}O$ solvent effects for the $H_2{}^{16}O_2$ derivatives of CcO, if measured, could provide a clue for the nature of these RR bands. In other words, the 355-cm^{-1} band assigned to a bending mode would be affected differently by the $H_2{}^{16}O/H_2{}^{18}O$ substitution, if it were due to the Fe−O stretching mode of the proposed Fe−O−O−H structure (Varotsis et al., 1993). Furthermore, comparison of these properties with other simple hemoproteins could provide an effective tool for evaluating the properties which are induced by Cu_B adjacent to Fe_{a3}.

Residues of the second type affect the kinetics of the reaction without interacting with the oxo oxygen directly. Since intensities of the oxygen-isotope-sensitive RR bands of the 580-nm form are altered around pH 8.5−9.0 under medium concentrations of peroxide (Figure 1), deprotonation of a residue with $pK_a = 8.5-9.0$ may slow down the overall reaction rate or facilitate the oxygen exchange, and as a result, the oxygen exchange exceeds the formation of the oxygen-labeled intermediates. Since the reaction still proceeds at pH 10.0 (Figure 2), protonation of the residue(s) with $pK_a = 8.5-9.0$ facilitates the reaction, but it is not a necessary condition. It should be noted that the two species of the 580-nm form behave somewhat differently in the pH range from 7.4 to 9.0.

Oliveberg et al. (1989) showed that two groups with pK_a 8.3 and 8.8 participate in the third and fourth phases, respectively, of the reaction of dioxygen with fully reduced CcO but not with mixed-valence CcO. They suggested that protonation of the group with $pK_a = 8.8$ must precede the transfer of the fourth electron to the binuclear center. This value is in remarkable agreement with the pH transition between 8.5 and 9.0 reported in this study. Involvement of one of distal histidines (His-283, His-333, and His-334) is plausible.

Implications of the Peroxide Reaction for the Dioxygen Reduction and Proton Pumping. The peroxide reaction has striking similarities to the dioxygen reduction in the following points: (1) Three oxo intermediates observed for the peroxide reaction by RR spectroscopy (Proshlyakov et al., 1996; this study) have the same frequencies as those in the dioxygen reaction (Han et al., 1990; Ogura et al., 1993; Varotsis et al., 1993). (2) Two intermediates, at least, were observed for the 580-nm form by RR spectroscopy (this study) and a similar multiplicity is suggested for the three-electron-reduced level in the dioxygen reaction (Blair et al., 1985; Oliveberg et al., 1991). (3) The same pH transition(s) was found in the peroxide reaction (this study) and the reaction of dioxygen with fully reduced but not with mixed-valence CcO (Oliveberg et al., 1989). (4) Identical absorption forms are found in the peroxide reaction and the reversed proton pumping for two separate intermediates (Wikström, 1989; Wikström & Morgan, 1992). (5) The peroxide reaction exhibits a sensitive H/D dependence in a certain step (this study) similar to the dioxygen reaction (Ogura et al., submitted for publication), implying that the enzyme pumps protons during the H_2O_2 reaction. These similarities indicate that the three intermediate species, that is, the 804-, 785-, and 355-cm^{-1} species, in the peroxide reaction are identical with the corresponding species which appear during the O_2 reduction. Thus, the [H_2O_2 + oxidized CcO] system is an excellent model for investigation of the physiological function of this enzyme.

REFERENCES

Babcock, G. T., & Wikström, M. (1992) *Nature 356*, 301−309.

Bickar, D., Bonaventura, J., & Bonaventura, C. (1982) *Biochemistry 21*, 2661−2666.

Blair, D. F., Witt, S. N., & Chan, S. I. (1985) *J. Am. Chem. Soc. 107*, 7389−7399.

Chan, S. I., & Li, P. M. (1990) *Biochemistry 29*, 1−12.

Fabian, M., & Palmer, G. (1995) *Biochemistry 34*, 13802−13810.

Gorren, A. C. F., Dekker, H., & Wever, R. (1986) *Biochim. Biophys. Acta 852*, 81−92.

Han, S., Ching, Y.-c., & Rousseau, D. L. (1990) *Nature 348*, 89−90.

Hashimoto, S., Tatsuno, Y., & Kitagawa, T. (1984) *Proc. Jpn. Acad. Ser. B 60*, 345−348.

Hashimoto, S., Nakajima, R., Yamazaki, I., Tatsuno, Y., & Kitagawa, T. (1986a) *FEBS Lett. 208*, 305−307.

Hashimoto, S., Tatsuno, Y., & Kitagawa, T. (1986b) *Proc. Natl. Acad. Sci. U.S.A. 83*, 2417−2421.

Hashimoto, S., Teraoka, J., Inubushi, T., Yonetani, T., & Kitagawa, T. (1986c) *J. Biol. Chem. 261*, 11110−11118.
Hosler, J. P., Ferguson-Miller, S., Calhoun, M. W., Thomas, J. W., Hill, J., Lemieux, L., Ma, J., Georgiou, C., Fetter, J., Shapleigh, J., Tecklenburg, M. M. J., Babcock, G. T., & Gennis, R. B. (1993) *J. Bioenerg. Biomembr. 25*, 121−136.
Kitagawa, T. (1986) in *Raman Spectroscopy of Biological Systems* (Clark, R. J. H., & Hester, R. E., Eds.) Vol. 13, pp 443−481, John Wiley and Sons, Chichester, U.K.
Kumar, C., Naqui, A., & Chance, B. (1984) *J. Biol. Chem. 259*, 11668−11671.
Malmström, B. G. (1985) *Biochim. Biophys. Acta 811*, 1−12.
Marchand, P., & Marmet, L. (1983) *Rev. Sci. Instrum. 54*, 1034.
Ogura, T., Takahashi, S., Hirota, S., Shinzawa-Itoh, K., Yoshikawa, S., Appelman, E. H., & Kitagawa, T. (1993) *J. Am. Chem. Soc. 115*, 8527−8536.
Oliveberg, M., Brzezinski, P., & Malmström, B. G. (1989) *Biochim. Biophys. Acta 977*, 322−328.
Oliveberg, M., Hallen, S., & Nilsson, T. (1991) *Biochemistry 30*, 436−440.
Orii, Y. (1988) *Ann. N.Y. Acad. Sci. 550*, 105−117.
Proshlyakov, D. A., Ogura, T., Shinzawa-Itoh, K., Yoshikawa, S., Appelman, E. H., & Kitagawa, T. (1994) *J. Biol. Chem. 269*, 29385−29388.
Proshlyakov, D. A., Ogura, T., Shinzawa-Itoh, K., Yoshikawa, S., & Kitagawa, T. (1996) *Biochemistry 35*, 76−82.
Reczek, C. M., Sitter, A. J., & Terner, J. (1989) *J. Mol. Struct. 214*, 27−41.
Sitter, A. J., Reczek, C. M., & Terner, J. (1985) *J. Biol. Chem. 260*, 7515−7522.
Spiro, T. G., Ed. (1988) *Biological Applications of Raman Spectroscopy*, Vol. 3, John Wiley & Sons, New York.
Terner, J., Sitter, A. J., & Reczek, C. M. (1985) *Biochim. Biophys. Acta 828*, 73−80.
Varotsis, C., Zhang, Y., Appelman, E. H., & Babcock, G. T. (1993) *Proc. Natl. Acad. Sci. U.S.A. 90*, 237−241.
Vygodina, T. V., & Konstantinov, A. A. (1988) *Ann. N.Y. Acad. Sci. 550*, 124−138.
Weng, L., & Baker, G. M. (1991) *Biochemistry 30*, 5727−5733.
Wikström, M. (1989) *Nature 338*, 776−778.
Wikström, M., & Morgan, J. E. (1992) *J. Biol. Chem. 267*, 10266−10273.
Wikström, M., Krab, K., & Saraste, M. (1981) *Cytochrome Oxidase: A Synthesis*, Academic Press, New York.
Wrigglesworth, J. M. (1984) *Biochem. J. 217*, 715−719.
Yoshikawa, S., Choc, M. G., O'Toole, M. C., & Caughey, W. S. (1977) *J. Biol. Chem. 252*, 5498−5508.

BI952096T